rare tautomers is likely to provide further useful information concerning the significance of tautomerism as a mechanism of mutation in nucleic acids.

Influence of Molecular Geometry on Tautomer Energetics. The use of molecular geometries determined in a minimal basis or by semiempirical methods followed by single-point energy evaluation in an extended basis has obvious computational advantages for the calculation of tautomer energetics. In Table X we show such results for C1-C6 using a MNDO optimized geometry followed by single-point 3-21G basis calculations (MNDO//3-21G). Similar results are shown in Table VII for U1 and U3 (STO-3G//3-21G). For cytosine, the largest errors (for C3 and C4) in the relative energies are $\sim$20 kJ mol^{-1} compared to our results using geometries optimized at the 3-21G level, although the order of stability of the tautomers is not altered. For U1 and U3 the STO-3G//3-21G calculations give an error of 11 kJ mol^{-1}, rather larger than the value of 1.2 kJ mol^{-1} found for the 2-pyridone/2-hydroxypyridine system.[28] These errors are considerably smaller than those resulting from the use of MNDO or STO-3G wave functions alone, both methods overestimating the stability of the lactim tautomer.

Basis Set Extension and Correlation Effects. We have not here considered larger basis sets than the 3-21G, nor the role of correlation effects. Geometry optimization of pyrimidine has been carried out by using a larger basis than that used here.[54] It was found that to obtain a comparable accuracy for the bond angles at nitrogen to that obtained for the angles at carbon, it was necessary to include polarization functions on the nitrogen atom. A similar effect is suggested from a comparison of the optimized structures obtained herein with the experimental geometries where the predicted CNC angles are too large by about 2°. Previous studies of 2-pyridone/2-hydroxypyridine and the corresponding 4-substituted isomers[28,29] suggest that the addition of polarization functions consistently favors the lactim tautomer by $\sim$10 kJ mol^{-1}. This is of particular significance for tautomer C3, for if it is stabilized relative to C1 by an additional 10 kJ mol^{-1} we would expect to observe it in the gas phase. However, calculations using Moller-Plesset perturbation theory[28] suggest that correlation effects favor the lactam tautomer by $\sim$5 kJ mol^{-1}.

(54) Pang, F.; Pulay, P.; Boggs, J. E. *J. Mol. Struct. (Theochem.)* **1982**, *88*, 79.

Conclusions

The major conclusions of the present theoretical study are the following: (1) Optimization at the 3-21G level yields molecular geometries in good agreement with average crystallographic values for uracil and cytosine, and superior to those previously obtained theoretically. (2) The most stable tautomers are predicted to be U1, T1, FU1, and C1 in agreement with experiment. The calculated relative energies of U1, U3, and U4 are in excellent agreement with experiment. (3) Substitution of uracil at the 5-position by CH_3 or F does not change the order of the stabilities of the tautomers. (4) The tautomeric equilibria of both uracil and cytosine are sensitive to phase change. (5) Use of the reaction field continuum model successfully explains the reordering of the relative tautomeric stabilities on passing from the gas phase to solution.

Registry No. Uracil, 66-22-8; cytosine, 71-30-7; thymine, 65-71-4; 5-fluorouracil, 51-21-8.

Influence of d-Orbital Occupancy on the Geometry of Pentacoordinated Molecules[1]

Robert R. Holmes

Contribution from the Department of Chemistry, University of Massachusetts, Amherst, Massachusetts 01003. *Received July 13, 1983*

Abstract: A quantitative assessment of solid-state structural data on five-coordinated compounds of both transition and main group elements establishes the geometrical change in the square pyramid as a function of d-orbital configuration. In terms of the trans basal angle θ, a variation in the range 140-174° is obtained. These angle variations are interpreted in terms of nonbonded repulsions between d-orbital electron density and bond electron density. Structural distortion from the trigonal-bipyramidal and square-pyramidal geometries are determined for the five-coordinated compounds by using a dihedral angle method. It is found that the local distortion coordinate for transition-metal complexes approximates the Berry intramolecular exchange coordinate. Main group pentacoordinated compounds follow this coordinate more closely.

It is known[2] that the square-pyramidal geometry assumed by some pentacoordinated phosphorus compounds has the phosphorus atom located out of the basal plane such that the trans basal angles, θ_{15} and θ_{24}, average 152°. This value was predicted by Zemann[3] on the basis of a point-charge model. X-ray investigations on a variety of five-coordinated phosphorus compounds further show that the structural form assumed varies from near the idealized trigonal bipyramid (TBP) to the square pyramid (SP).[2,4] These structures lie along a C_{2v} coordinate connecting the two limiting geometries and are supportive of the Berry pseudorotation mechanism[5] frequently invoked[6] to interpret dynamic NMR data indicative of intramolecular ligand exchange.

Although a great deal of structural work has been reported for five-coordinated transition-metal compounds, no quantitative assessment of the "preferred" geometry of the square-pyramidal form is available. The literature contains isolated references of possible variations. For example, high- and low-spin square-pyramidal Co(II) and Ni(II) complexes have been classified by Orioli[7] in terms of metal atom displacement from the basal plane.

(1) Pentacoordinated Molecules. 55. Previous paper in the series: Deiters, J. A.; Holmes, R. R. *J. Am. Chem. Soc.* **1984**, *106*, 3307-3309.
(2) Holmes, R. R. *ACS Monogr.* **1980**, *175*, 44.
(3) Zemann, J. *Z. Anorg. Allg. Chem.* **1963**, *324*, 241.
(4) Holmes, R. R.; Deiters, J. A. *J. Am. Chem. Soc.* **1977**, *99*, 3318.
(5) Berry, R. S. *J. Chem. Phys.* **1960**, *32*, 933.
(6) See ref 2, Chapter 3.
(7) Orioli, P. L. *Coord. Chem. Rev.* **1971**, *6*, 285.

0002-7863/84/1506-3745$01.50/0

Table I. Dihedral Angle Differences for Square-Pyramidal θ Values

θ, deg	$S = \sum_i \lvert\delta_i(\text{TBP}) - \delta_i(\text{SP})\rvert$, deg
140	209.2
145	213.4
150	217.7
160	226.5
170	235.6
174	239.3

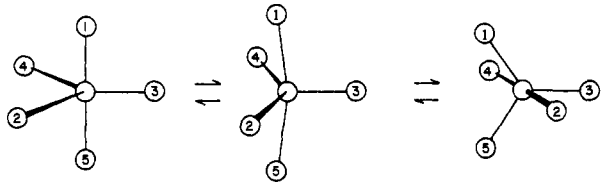

Figure 1. Berry intramolecular ligand exchange process.

It is of interest to learn to what extent the geometry of the square pyramid changes across a transition series as the d configuration varies from d^0 to d^{10}. This paper treats this main feature of pentacoordinated compounds for both transition metals and main group derivatives. A rationale is offered for the observations in terms of variations in bonding attributed to changes in d-orbital configuration.

Structural Distortion

Calculations. Sufficient structural data on five-coordinated complexes, largely from X-ray diffraction studies,[8] are available for many of the transition elements to provide a basis for the treatment here. Similar to that formed with pentacoordinated phosphorus compounds, the transition-metal derivatives have structures that usually are intermediate in geometry between the trigonal bipyramid and the square pyramid. Adopting the procedure we used with phosphorus compounds,[2,4,9] transition-metal structures may be interpreted in two ways. In one method,[4] dihedral angles are calculated from the triangular faces of the polyhedron established by the positions of the five ligands attached to the metal. If these values are compared with the related values of the dihedral angles for the idealized trigonal bipyramid and square pyramid and their differences obtained, a measure of the structural distortion between these two forms may be established. The sum of the respective dihedral angle changes between the two idealized geometries $\sum_i \lvert\delta_i(\text{TBP}) - \delta_i(\text{SP})\rvert$ provides a common scale to compare structures of various five-coordinated compounds. The value of this sum is 217.9° when the trans basal angle θ for the reference square pyramid is 150°. Whenever the reference square pyramid has a different trans basal angle, it is necessary to recalculate this sum. These are given in Table I for square pyramids which have θ values that range from 140° to 174°.

A less elaborate procedure[4] is to make use of the values of the axial and equatorial angles, θ_{15} and θ_{24}, respectively, relative to the dihedral angle δ_{24} as a measure of the distortion coordinate, a method first applied to acyclic five-coordinated transition metals by Muetterties and Guggenberger.[10] The dihedral angle δ_{24} is the angle formed between normals to the trigonal-bipyramidal faces 124 and 245 that have the common equatorial edge 24 and is the one most intimately associated with the Berry exchange coordinate (Figure 1). This dihedral angle has a value of 53.1° for an idealized trigonal bipyramid but becomes 0° as edge 24 disappears on forming the square pyramid. Application of these methods to phosphorane compounds[2,9] has shown close adherence to the Berry ligand exchange coordinate in their structural distortions between the two reference five-coordinated geometries. A θ value of 152° is obtained for the limiting square pyramid.

(8) Holmes, R. R. *Prog. Inorg. Chem.*, in press.
(9) Holmes, R. R. *Acc. Chem. Res.* **1979**, *12*, 257.
(10) Muetterties, E. L.; Guggenberger, L. J. *J. Am. Chem. Soc.* **1974**, *96*, 1748.

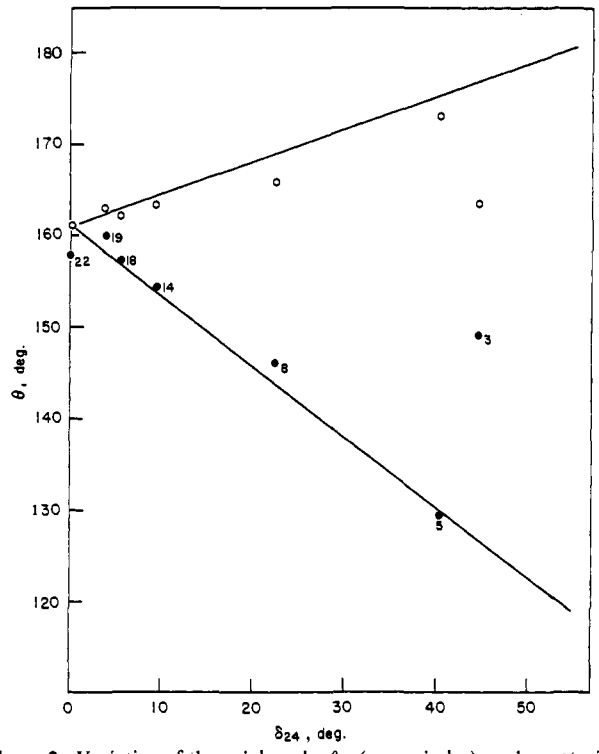

Figure 2. Variation of the axial angle, θ_{15} (open circles), and equatorial angle, θ_{24} (filled circles), vs. the dihedral angle, δ_{24}, as structural distortion for pentacoordinated high-spin nickel(II) compounds proceeds along a Berry type coordinate from a square pyramid toward a trigonal bipyramid. The numbers refer to specific compounds given in ref 8.

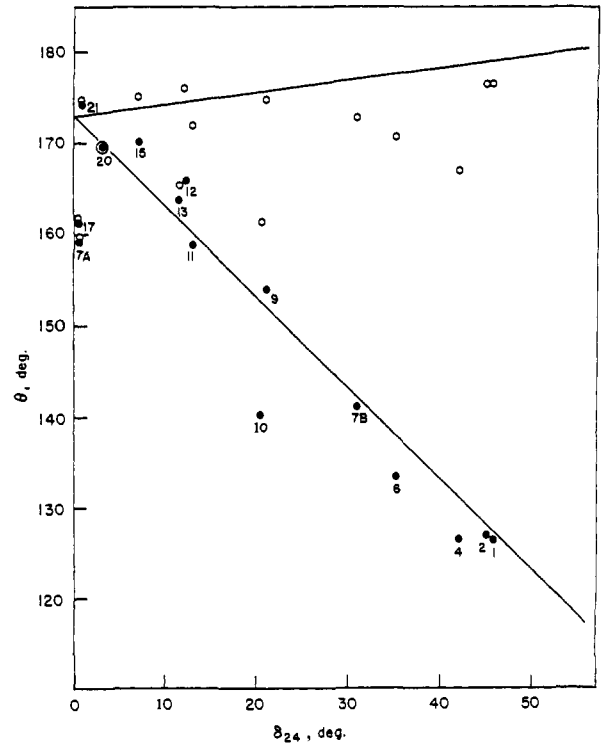

Figure 3. Variation of the axial angle, θ_{15} (open circles), and equatorial angle, θ_{24} (filled circles), vs. the dihedral angle, δ_{24}, as structural distortion for pentacoordinated low-spin nickel(II) compounds proceeds along a Berry type coordinate from a square pyramid toward a trigonal bipyramid. The numbers refer to specific compounds given in ref 8.

Preferred Square-Pyramidal Geometries

By construction of graphs of θ_{15} and θ_{24} vs. δ_{24} for five-coordinated compounds of other elements in a given oxidation state, preferred square-pyramidal geometries may be established which

Table II. Oxidation States of Elements Identified by Points in Figure 7[a]

d^n, n =										
0	1	2	4	4.5	5	6	7	8	9	10
1, ^{10}Si(IV)	3, ^{1}W(V)	6, ^{2}Mo(IV)	9, ^{2}Mo(II)	12, ^{1}Tc[b]	13, ^{1}Co(IV)	16, ^{2}Co(III)	20, ^{6}Co(II)	22, ^{11}Ni(II)	25, ^{30}Cu(II)	26, ^{1}Hg(II)
1, ^{56}P(V)	4, ^{9}V(IV)	7, ^{2}Tc(V)	10, ^{1}Tc(III)		14, ^{2}Mn(II)	17, ^{5}Rh(III)	21, ^{6}Co(II)	23, ^{4}Pt(II)		26, ^{4}Sn(IV)
1, ^{1}Mo(VI)	5, ^{4}Mo(V)	8, ^{1}Os(VI)	11, ^{2}W(II)		15, ^{5}Fe(III)	18, ^{3}Ir(III)		24, ^{6}Ni(II)		27, ^{13}Ge(IV)
2, ^{1}W(VI), ^{6}Ta(V)						18, ^{1}Fe(II)				27, ^{9}As(V)
										27, ^{3}In(III)
						19, ^{4}Ru(II)				27, ^{5}Sb(V)
										28, ^{3}Cd(II)

[a] A number followed by the oxidation state(s) of the five-coordinated complexes that are plotted in Figure 7 is listed here. A superscript on the element indicates the number of compounds used in establishing a particular point. [b] This entry corresponds to a formal oxidation state of 2.5.

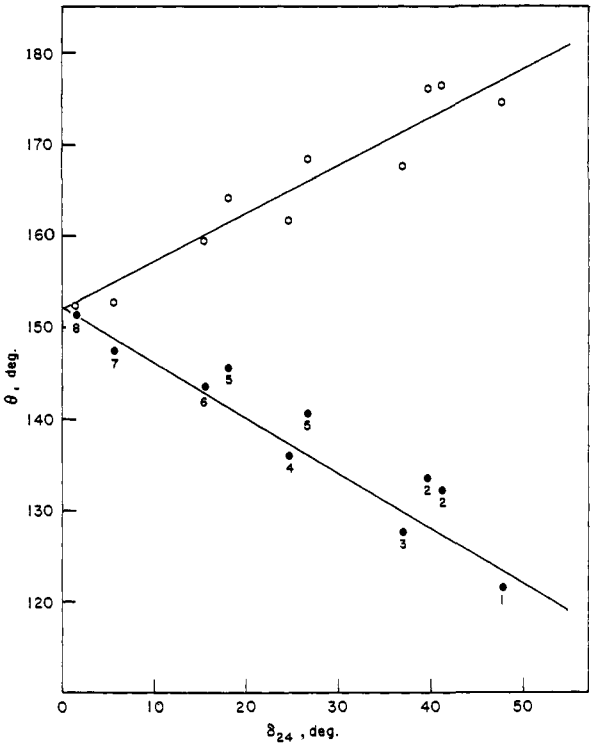

Figure 4. Variation of the axial angle, θ_{15} (open circles), and equatorial angle, θ_{24}, (filled circles), vs. the dihedral angle, δ_{24}, as structural distortion for pentacoordinated silicon(IV) compounds proceeds along the Berry coordinate from a square pyramid toward a trigonal bipyramid. The numbers refer to specific compounds given in ref 8.

should reveal interesting variations with changes in d-orbital configurations. To accomplish this, crystal structure data were analyzed[11] by making use of the bond angles between the ligands directly connected to the central atom.

Figures 2 and 3 show θ vs. δ_{24} plots for high- and low-spin Ni(II) compounds, respectively. A similar graph is given in Figure 4 for Si(IV) five-coordinated compounds. From these graphs, the θ value for δ_{24} equal to zero is determined. As with cyclic phosphoranes, the best θ value for a square-pyramidal pentacoordinated silicon(IV) compound is 152°. For Ni(II) there is a considerable difference in the ideal θ value to use for a low-spin square-pyramidal nickel complex (θ = 173°) compared to a high-spin nickel complex (θ = 161°). Although high-spin Ni(II) compounds available here are more sparse than their low-spin counterparts, the members span the range between the trigonal bipyramid and square pyramid in each case with the low-spin members perhaps displaying a more even distribution. The high-spin members show a slight preference for the square pyramid. A concentration toward the square pyramid is favored for high-spin d^8 five-coordinated complexes on the basis of the angular overlap model.[12]

(11) This analysis is given in full in ref 8.
(12) Purcell, K. F.; Kotz, J. C. "Inorganic Chemistry"; Saunders: Philadelphia, 1977; p 587 ff.

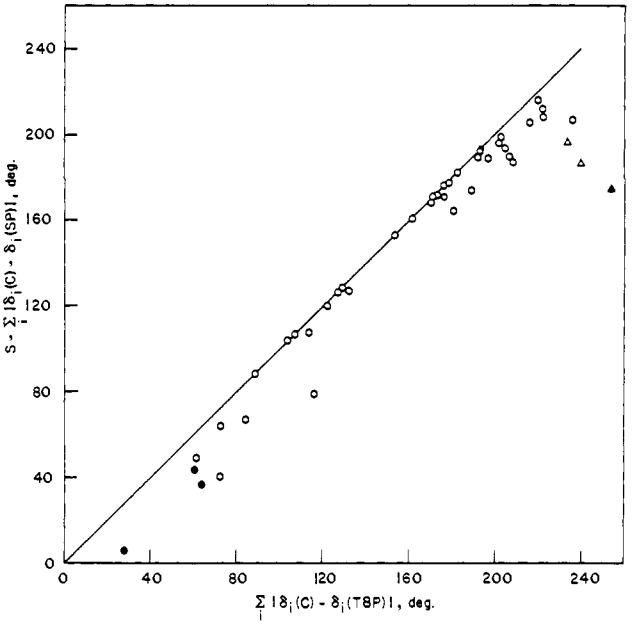

Figure 5. Sum of dihedral angles for pentacoordinated copper(II) compounds from a square-pyramidal geometry vs. the sum from a trigonal bipyramid on a common reference scale. Compounds containing tripodal ligands (filled circles), constrained ligand systems (open triangles), or have hydrogen bonding present (filled triangle) are considerbly displaced from the Berry coordinate.

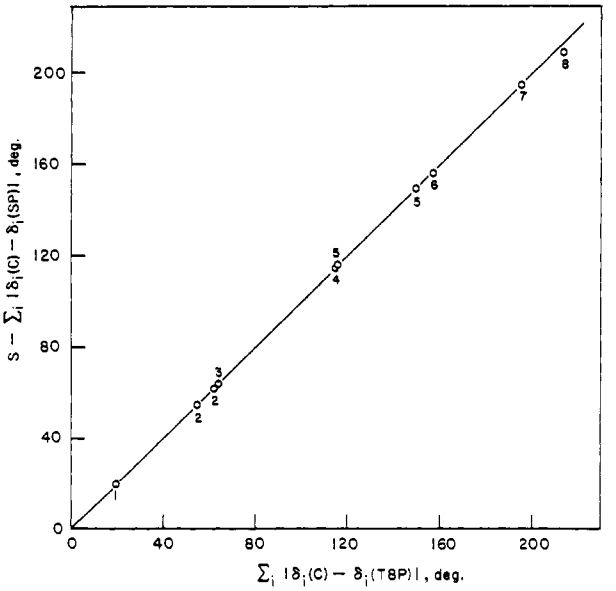

Figure 6. Sum of dihedral angles for pentacoordinated silicon(IV) compounds from a square-pyramidal geometry vs. the sum from a trigonal bipyramid on a common reference scale. The numbers refer to specific compounds given in ref 8.

Dihedral angle plots for five-coordinated compounds of Si(IV) and Cu(II) are given in Figures 5 and 6, respectively. These plots

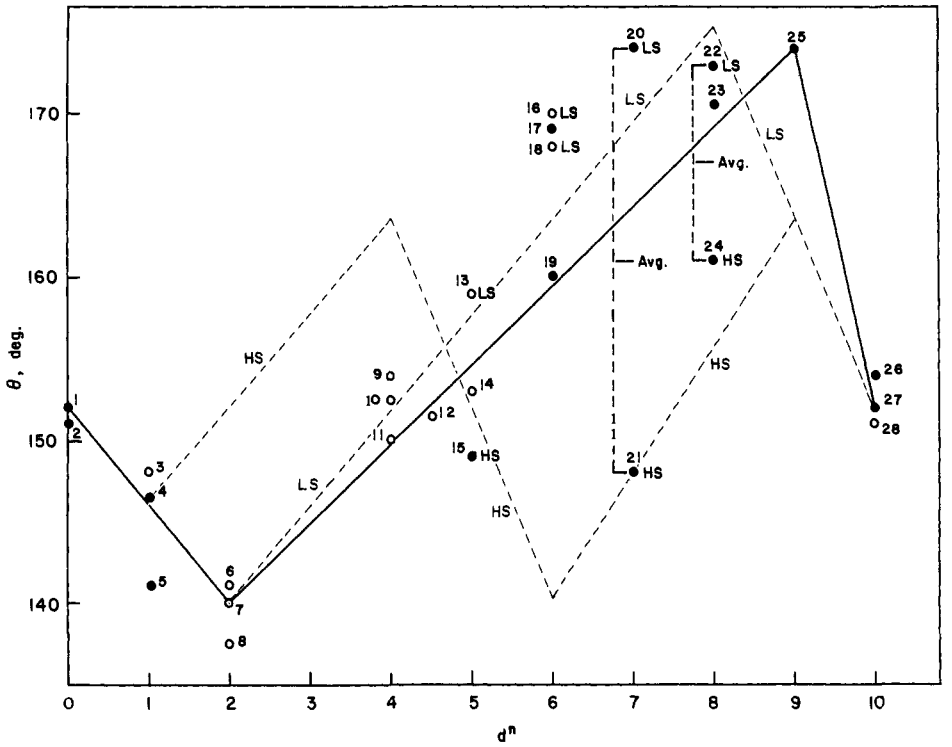

Figure 7. Variation of the trans basal angle θ for preferred square pyramids vs. the d-orbital configuration (d^n) of the central element for pentacoordinated compounds. The points are identified in Table II. Filled circles refer to points determined with four or more compounds. Open circles refer to points based on three or less compounds. LS = low spin. HS = high spin. The solid line represents the general trend of θ vs. d^n. The light dashed line is a superposition of Figure 10 representing a model description which differentiates between high-spin and low-spin systems.

show close adherence of the Berry pseudorotational coordinate[5] even more so than the θ plots.

Treating crystallographic data in a similar fashion for other five-coordinated elements results in the determination of preferred square pyramids from the basis set used. The θ values determined in this way are included in graphical form in Figure 7 as a function of d-orbital configuration. In Table II, each point shown in Figure 7 is identified in terms of the responsible pentacoordinated elements and their oxidation states.

As the d-orbital occupancy increases (starting at d^0 with θ = 152°) for the various five-coordinated transition elements, the limiting square pyramid at first becomes more pyramidal. At d^2, θ is near 140° where a reversal in θ takes place. From d^2 to d^9 there is a gradual flattening of the square pyramid as θ rises from 140°, passing near 150° for high-spin d^5 Fe(III), and up to 174° for d^9 Cu(II). When d^{10} is reached, an abrupt decrease in θ to 152° is apparent as the limiting square pyramid returns to the starting configuration. Although the average values of θ for the cobalt(II) and nickel(II) structures follow this trend, the low-spin derivatives show a much higher θ value than that for the high-spin complexes, as already mentioned.

Discussion

Repulsion Model. The variation in the trans basal angle as a function of d-orbital configuration, displayed in Figure 7, may be interpreted simply from the relative order of d-orbital energy levels of the square pyramid. For this purpose, it is instructive to refer to the energy correlation diagram along the pseudorotational coordinate connecting the trigonal bipyramid and square pyramid. Figure 8 portrays this coordinate[13] and includes the symmetry changes encountered. In contrast to the D_{3h} trigonal bipyramid where d-orbital occupancy will exert a primary influence on relative bond lengths, the additional angular parameter present in the C_{4v} square pyramid allows d-orbital effects to be reflected in both bond distance and bond angle variations. It is reasonable that bond angle changes should preferentially occur in the absence of other controlling factors since less energy normally is required for bond bending compared to bond stretching.

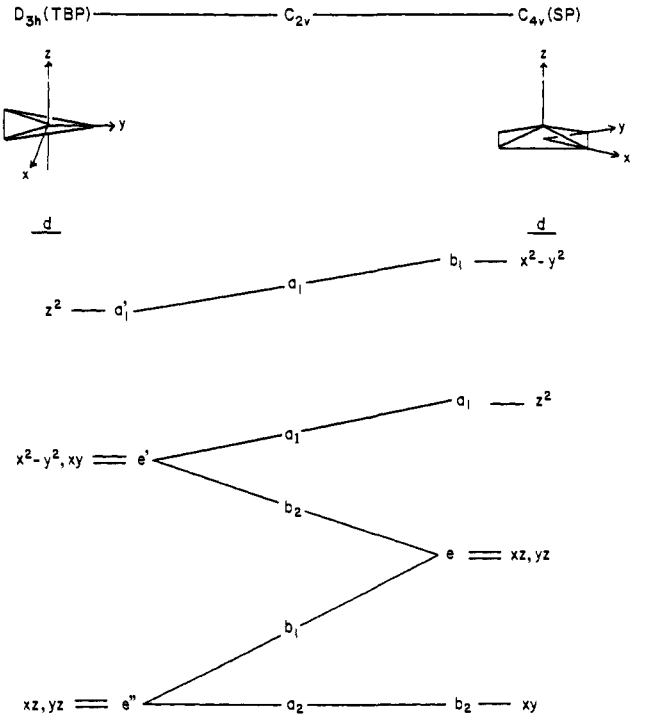

Figure 8. Relative d-orbital energy levels connecting the trigonal bipyramid and square pyramid along the Berry pseudorotation coordinate.[13] The relative energy levels are appropriate for the range of structures considered here.[13]

In the model that follows, the interpretation of θ changes for square pyramids is given in terms of repulsions between nonbonding electrons in occupied d orbitals, largely antibonding with respect to the ligands in the MO scheme, and bond electron density.

The repulsion effects are seen more readily if the d orbitals are viewed in the square-pyramidal reference frame (Figure 9). Considering the low-spin case first, in the absence of π bonding

(13) Rossi, A. R.; Hoffmann, R. *Inorg. Chem.* **1975**, *14*, 365.

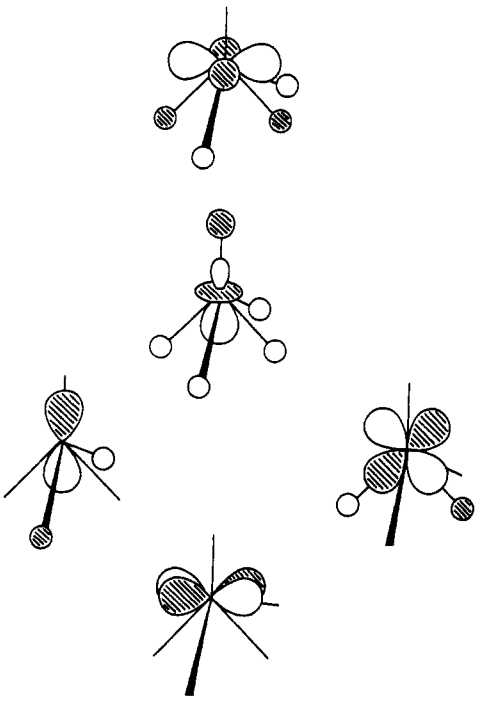

Figure 9. Antibonding d orbitals ascending in increasing energy in a square-pyramidal geometry. Although the relative energies will modify somewhat as θ changes, there are no crossovers for the θ range, 140–174°, based on an extended-Hückel treatment.[13]

and starting at d^0 with $\theta \cong 152°$, the addition of nonbonding electrons to the lowest energy d_{xy} orbital causes a repulsion with the basal bond electron pairs which could be relieved by further lengthening of the basal bonds or preferentially by a decrease in θ since this electron density resides above the basal plane. In contrast, the occupancy of the e level, even with a uniform electron distribution in either the antibonding d_{xz} or d_{yz} orbital, would cause a repulsion with the basal bond electron density resulting in an expansion of θ. A similar unbalanced repulsion effect occurs at the a_1 level as the z^2 level is occupied, giving rise to an additional increase in θ toward 180°. Filling the $d_{x^2-y^2}$ orbital corresponding to the b_1 level, like the d_{xy} level, produces a repulsion which now decreases θ. Completion of the d shell at d^{10} once again gives a uniform d electron density resulting in a square-pyramidal configuration similar to d^0 with θ back to 152°.

For the high-spin case, following the same reasoning in terms of repulsion effects between electron pairs in basal bonds and d-orbital electron density, θ should rise from d^1 to d^4 as the e and a_1 levels are singly occupied. As an additional electron is added, giving d^5, θ returns to the value for d^0. At d^6, where the d_{xy} level is filled, θ continues the downward trend. θ then is expected to increase from d^6 to d^9 as the e and a_1 levels fill, paralleling the θ increase between d^1 and d^4.

These changes in the square-pyramidal geometry expected from this model are summarized graphically in Figure 10. It reproduces the main structural changes experimentally encountered (Figure 7) other than the drop in θ expected on going from low-spin d^8 to the d^9 configuration. The model graph in Figure 10 is constructed by using the θ range observed for square-pyramidal compounds, i.e., 140–175°. With θ for d^0, d^{10}, and high-spin d^5 at 152°, θ for d^9 is established as ~163°. This value is also used for the peak in θ for high-spin d^4. Superposition of Figure 10 on Figure 7 by way of dashed lines shows the degree of agreement with the experimental data.

With this model, the much higher values for θ for low-spin Co(II) and Ni(II) complexes compared to their high-spin counterparts is easily rationalized. Transfer of a nonbonding d electron from the $d_{x^2-y^2}$ orbital to either the e level for Co(II) or the a_1 level for Ni(II), on going from high to low spin, transfers electron density from the region above (toward the apical ligand) the metal–basal ligand bonds to the region below these bonds.

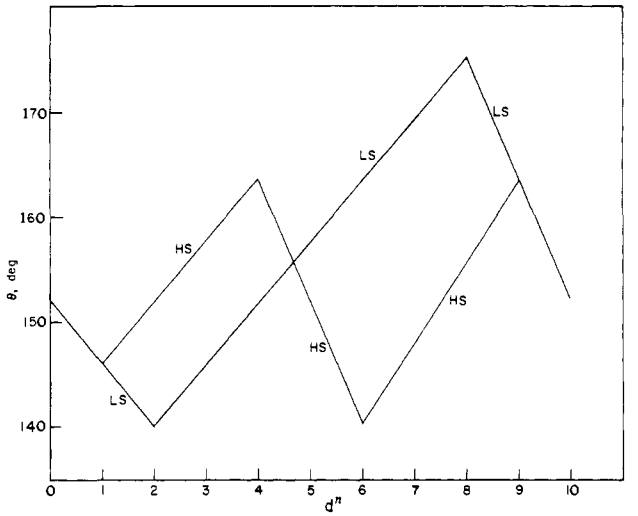

Figure 10. Repulsion model description of the variation of the trans basal angle θ of the square pyramid vs. d-orbital configuration (d^n) of the central element of pentacoordinated compounds. HS = high spin. LS = low spin.

Consequently, an increase in θ is expected, consistent with the sizeable change observed in each case. Other low-spin complexes are displaced equally to the high θ side of the average trend given in Figure 7, e.g., low-spin d^6 Co(III).

If π bonding effects are considered, we should expect some modification from the model just presented. Following Rossi and Hoffmann,[13] some reduction of the nonbonding d electron density is expected to account for the mixing of antibonding d character into basal bonds (via e and b_1 orbitals) or into the apical bond (via the a_1 orbital) in σ-bond formation and, in the case of π bonding, mixing d character into basal bonds from the xz, yz, z^2, and xy orbitals and xz and yz character into the apical bond. It is noted that all of the d^1 and d^2 square-pyramidal complexes used to construct Figure 9 have apical π-donor ligands which should add electron density to the xz and yz orbitals that are then hybridized toward the apical ligand. Repulsion of this electron density and the basal electron pairs should help to lower θ.

Many low-spin d^7 and d^8 square-pyramidal complexes have strong basal π-acceptor ligands and only weakly σ-bonding apical ligands.[7] This should reduce electron density preferentially in the d_{xy} orbital in forming the π-bond system and increase electron pair bond repulsion among the strongly covalent basal bonds, both effects tending to increase θ. At d^9, the expected drop in θ value is not experimentally observed (Figure 7). Perhaps, because the $d_{x^2-y^2}$ orbital is the highest energy orbital and is involved most strongly in metal-basal ligand antibonding, the repulsion effect is not as effective as the others.

Bond Parameters. Concerning the latter point, it is instructive to examine bond distance values for pentacoordinated derivatives that have identical ligands bonded to the different positions of either the trigonal bipyramid or square pyramid. Although the major trends follow those set forth by Rossi and Hoffmann,[13] the d^9 configuration provides an exception.

It is generally found[8] that square-pyramidal copper(II) complexes have apical bonds that average about 0.35 Å longer than basal central atom–ligand distances. The difference between bond lengths that can be classified as equatorial relative to those that are axial for the trigonal-bipyramidal structural type for copper(II) complexes is about 0.15 Å, with the equatorial bonds having the greater length.

Pentacoordinated d^8 low-spin nickel(II) complexes follow the same pattern.[8] For these nickel(II) complexes containing like ligands, however, the differences are smaller. The nickel complexes exhibiting axial–equatorial character of the trigonal bipyramid over the observed spectrum of structural distortions (Figures 2 and 3) have nickel–ligand equatorial distances which average about 0.05 Å longer than the respective axial distances. Apical distances in the square pyramid are approximately 0.2 Å longer than

nickel-ligand basal distances. Bond distance data[8] for high-spin nickel(II) square pyramid show slightly longer basal bonds relative to apical bonds, averaging a few hundredths of an angstrom longer.

While it is expected[13] that d^8 low-spin five-coordinated complexes follow the observed pattern for relative bond lengths in the two geometrical types, d^9 complexes should follow this pattern to a lesser degree, not to a greater degree as observed for copper(II). Possibly, the addition of an electron to the SP b_1 level, which is strongly metal-basal ligand antibonding, serves to lengthen the apical copper-ligand bond rather than to decrease the trans basal angle θ. This could occur if the $x^2 - y^2$ orbital mixes in an antibonding way with basal ligand orbitals for copper complexes and as a consequence results in a destabilization of the b_1 level and hydridization away from the basal ligands toward the apical site. With considerable basal π bonding for copper complexes enhancing bond electron pair repulsions, this would rationalize the high θ value maintained for square-pyramidal copper(II) complexes (Figure 7).

As a final point, both the θ distortion coordinates and the dihedral angle coordinates suggest that the concerted axial-equatorial bending process is a predominant feature in assessing molecular distortions for five-coordinated derivatives. Further, the ease of distortion along these coordinates, whether by relief of ligand ring strain, steric effects, particular electronic properties of ligands, or lattice effects, implies that they represent a basis for stereochemical nonrigidity prevalent in solution for some five-coordinated members. Although structures of transition-metal derivatives tend to concentrate more readily toward the square pyramid for many of the elements, particularly d^6 complexes, there is a distribution covering the range between the two idealized limits in most cases. The preference of low-spin d^6 complexes for the square pyramid is supported by both the angular overlap model[12] and the relative ordering of energy levels in Figure 8.[13]

Acknowledgment. The support of this research by the National Science Foundation (CHE 8205411) is greatly appreciated. I am extremely grateful to Professor Roberta O. Day and Joan M. Holmes, who carried out the calculations on structural distortions.

Anionic Group 6B Metal Carbonyls as Homogeneous Catalysts for Carbon Dioxide/Hydrogen Activation. The Production of Alkyl Formates

Donald J. Darensbourg* and Cesar Ovalles

Contribution from the Department of Chemistry, Texas A&M University, College Station, Texas 77843. *Received November 2, 1983*

Abstract: The production of alkyl formates from the hydrocondensation of carbon dioxide in alcohols utilizing anionic group 6B carbonyl hydrides as catalysts is herein reported. $HM(CO)_5^-$ (M = Cr, W; derived from μ-$H[M_2(CO)_{10}]^-$) and their products of carbon dioxide insertion, $HCO_2M(CO)_5^-$, have been found to be effective catalysts for the hydrogenation of CO_2 in alcohols under rather mild conditions (loading pressures of CO_2 and H_2, 250 psi each, and 125 °C) to provide alkyl formates. The only metal carbonyl species detected in solution via infrared spectroscopy, both at the end of a catalytic period and during catalysis, were $M(CO)_6$ and $HCO_2M(CO)_5^-$. The metal hexacarbonyls were independently shown to be catalytically inactive. A catalytic cycle is proposed which initially involves release of formic acid from the metal center, either by reductive elimination of the hydrido formato ligands or ligand-assisted heterolytic splitting of dihydrogen with loss of formic acid. In a rapid subsequent process HCOOH reacts with alcohols to yield HCOOR. The addition of carbon monoxide retards alkyl formate production, strongly implying CO_2 to be the primary source of the carboxylic carbon atom in HCOOR. This was verified by carrying out reactions in the presence of $HCO_2W(^{13}CO)_5^-$ which provided *only* $H^{12}COOR$ after short reaction periods. However, in the *absence of hydrogen and carbon dioxide* μ-$H[M_2(CO)_{10}]^-$ species were observed to be effective catalyst precursors for converting CO and methanol into methyl formate.

The anionic metal carbonyl hydrides of the group 6B metals have been shown to reversibly bind carbon dioxide with concomitant formation of metalloformate derivatives (eq 1).[1-3] The

$$HM(CO)_5^- + CO_2 \rightleftharpoons HCO_2M(CO)_5^- \qquad (1)$$

forward reaction, i.e., the insertion of carbon dioxide into the metal-hydrogen bond, occurs instantaneously even at low pressures of carbon dioxide (<760 torr); however, the reverse process, decarboxylation, proceeds at ambient temperature only in the case where M = Cr.

On the other hand, the $HCO_2M(CO)_5^-$ species all undergo facile CO ligand substitution reactions with ^{13}CO, a process which occurs stereoselectively at the cis (equatorial) CO sites (eq 2). This is

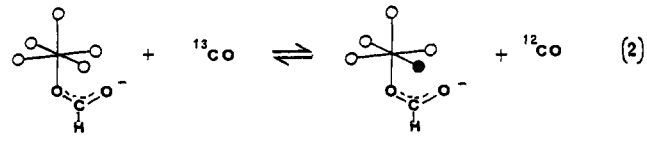

(2)

in fact a feature common to a large variety of O-bonded metal entities,[4] and it is a process of importance in the decarboxylation pathway, i.e., excess carbon monoxide retards the extrusion of CO_2

(1) Darensbourg, D. J.; Rokicki, A.; Darensbourg, M. Y. *J. Am. Chem. Soc.* **1981**, *103*, 3223.
(2) Darensbourg, D. J.; Rokicki, A. *ACS Symp. Ser.* **1981**, *152*, 107.
(3) Darensbourg, D. J.; Rokicki, A. *Organometallics* **1982**, *1*, 1685.
(4) (a) Darensbourg, D. J.; Walker, N.; Darensbourg, M. Y. *J. Am. Chem. Soc.* **1980**, *102*, 1213. (b) Darensbourg, D. J.; Darensbourg, M. Y.; Walker, N. *Inorg. Chem.* **1981**, *20*, 1918. (c) Darensbourg, D. J.; Fischer, M. B.; Schmidt, R. E., Jr.; Baldwin, B. J. *J. Am. Chem. Soc.* **1981**, *103*, 1297. (d) Cotton, F. A.; Darensbourg, D. J.; Kolthammer, B. W. S. *Ibid.* **1981**, *103*, 398. (e) Cotton, F. A.; Darensbourg, D. J.; Kolthammer, B. W. S.; Kudaroski, R. *Inorg. Chem.* **1982**, *21*, 1656. (f) Darensbourg, D. J.; Pala, M.; Waller, J. *Organometallics* **1983**, *2*, 1285.

0002-7863/84/1506-3750$01.50/0